Molecular Multicolor Multiphoton in Vivo Bioimaging Based on a Direct Diode Pumped Ti:sapphire Oscillator

Marco Andreana, Caterina Sturtzel, Ming Yang, Richard Latham, Rainer A. Leitgeb, *Member, IEEE*, Wolfgang Drexler, Manuel Zimmer, Tuan Le, Martin Distel, and Angelika Unterhuber

***Abstract*—Multiphoton microscopy (MPM) including two-photon excited fluorescence (TPEF), second harmonic generation (SHG), coherent anti-Stokes Raman scattering (CARS) is an important tool in biology and medicine to explore the dynamics of cells and to investigate tissue structure in living systems and biopsies. However, MPM still suffers from limited applicability due to the integration of highly sophisticated lasers. In this paper, we introduce our triple-modal multicolor MPM platform employing a single direct diode-pumped femtosecond Kerr-lens-mode-locked Ti:sapphire oscillator and acquire simultaneously intrinsic co-registered multicolor TPEF, TPEF, SHG and CARS signals in the backward direction. The complexity and by that the footprint as well the cost of the laser are considerably reduced by the direct diode-pumping scheme. In combination with an Yb fiber amplifier such a laser is suited for biomedical applications allowing for detailed morphologic and molecular spectroscopic in vivo investigation. The optimized emission wavelengths of our Ti:sapphire laser and Yb fiber amplifier provide simultaneous excitation at 805 nm, 1050 nm and 911 nm for multicontrast information from exogenous and endogenous fluorophores. We perform in vivo imaging of *C. elegans* and visualize metabolic changes in zebrafish larvae to investigate the tumor microenvironment with spectral focusing CARS and multicolor TPEF of green fluorescent protein.**

***Index Terms*—Biomedical microscopy, biomedical optical imaging, fluorescence, laser applications, light sources, mode locked lasers, nonlinear optics, raman scattering.**

Manuscript received November 20, 2020; revised February 12, 2021; accepted February 12, 2021. Date of publication February 22, 2021; date of current version March 17, 2021. This work was supported in part by the Austrian Science Fund (FWF) [I 4166-B], in part by the European Union's Seventh Framework Programme (FAMOS, FP/-ICT-2011-3-5-a) under Grant FP7-ICT-317744, and in part by the Austrian Research Promotion Agency (FFG) project 7940628 (Danio4Can). *(Corresponding author: Angelika Unterhuber.)*

Marco Andreana, Rainer A. Leitgeb, Wolfgang Drexler, and Angelika Unterhuber are with the Center for Medical Physics and Biomedical Engineering, Medical University of Vienna, Vienna 1090, Austria (e-mail: marco.andreana@meduniwien.ac.at; rainer.leitgeb@meduniwien.ac.at; wolfgang.drexler@meduniwien.ac.at; angelika.unterhuber@meduniwien.ac.at).

Caterina Sturtzel and Martin Distel are with the Innovative Cancer Models, St. Anna Children's Cancer Research Institute, Vienna 1090, Austria (e-mail: caterina.sturtzel@ccri.at; martin.distel@ccri.at).

Ming Yang and Tuan Le are with the VIULASE GmbH, Vienna 1230, Austria (e-mail: ming.yang@viulase.com; tuan.le@viulase.com).

Richard Latham and Manuel Zimmer are with the Department of Neuroscience and Developmental Biology, University of Vienna, Vienna 1090, Austria, and also with the Research Institute of Molecular Pathology (IMP), Vienna Biocenter (VBC), Vienna 1030, Austria (e-mail: richard.latham@imp.ac.at; manuel.zimmer@imp.ac.at).

Color versions of one or more figures in this article are available at https://doi.org/10.1109/JSTQE.2021.3060289.

Digital Object Identifier 10.1109/JSTQE.2021.3060289

I. Introduction

UNDERSTANDING the dynamics of metabolism in multicellular organisms is important in unraveling the mechanism behind many biological processes, i.e. tumor development [1]. Although state-of-art technologies can catalog thousands of biomarkers residing in cells, non-destructive and non-invasive tools are limited for visualization of metabolic activities, such as protein and lipid synthesis at (sub)cellular resolution in living organisms [2]. Multiphoton microscopy (MPM) is a powerful tool for non-invasive functional imaging and has emerged as ubiquitous imaging tool in many areas of the life sciences [3], [4]. Especially its significance in neuroscience is undisputable and the pioneers of the first MPM work were awarded with the Brain Prize in 2015. MPM include two-photon excited fluorescence (TPEF) microscopy, second harmonic generation (SHG) microscopy [5], and coherent anti-Stokes Raman scattering (CARS) microscopy [6] amongst other modalities. Each MPM technique provides unique structural and or molecular contrast, but shares the same concept of non-linear optical imaging. MPM uses non-ionizing radiation with the potential of in vivo assessment of structural, functional, metabolic and molecular features in pathological conditions in a harmless way with multiple interaction mechanisms. It provides submicron isotropic spatial resolution with intrinsic three dimensional sectioning as well as minimal photo-damage, reduced photo-toxicity and enhanced penetration depth due to the use of near infrared (NIR) light [7]. Multimodal imaging can be performed with different image contrasts for screening [8], diagnosis and interventional guidance [9], [10] in addition to effective monitoring of disease progression and treatment response [11]. Fluorescence from endogenous and exogenous molecules can be excited with TPEF in living specimen based on simultaneous absorption of two photons. Indeed, fluorescent proteins have rather large two-photon cross-section and are hence increasingly used for studies of live tissues. With the availability of many spectral variants of fluorescent proteins, researchers are interested in simultaneous imaging of multiple biomarkers to clarify the dynamic interactions at molecular level. Nowadays, this is possible by using complicated imaging systems based on several excitation lasers and several detectors or by rapid changing of wavelength of an ultra-short pulse laser which is not practical [12]–[15]. Moreover, living organisms

cannot be studied only relying on endogenous or exogenous proteins but a combination of them is required when dealing with complex biological systems, such as small animals. Indeed, the number of exogenous molecules that can be inserted in the cells are limited in terms of spectral cross-talk and might interfere with the metabolic activities.

Recent advances in fluorescence microscopy are remarkable. TPEF microscopy is the most common and widespread implementation of MPM. This technique visualizes exogenous and endogenous fluorophores related to electronic transition from the excited to the ground state of a molecule by two-photon excitation and related molecule-specific fluorescent emission of a photon from a lower energy emissive state [3]. Unprecedented sensitivity is offered due to the intense electronic transition dipole moment. Intracellular or extracellular tissue autofluorescence from vitamins (or vitamin derivatives) such as retinol, cholecalciferol, riboflavin or pyridoxine emitting in the visible or aromatic amino acids including tyrosine, phenylalanine and tryptophan emitting in the UV can be used to investigate biochemical and metabolic changes. Intracellular endogenous fluorophores such as nicotinamide adenine dinucleotide (NADH) and its phosphate derivative (NADPH), and flavins as flavin adenine dinucleotide (FAD) are important biomarkers associated with cellular metabolism. Extracellular endogenous fluorophores such as collagen and elastin form the extracellular matrix (ECM), which is altered in many pathologies and also involved in remodeling of the tumor microenvironment during tumorigenesis [16]. In addition, a wealth of exogenous fluorescent labels is available for tissue that is intrinsically non-fluorescent or only weakly fluorescent. To provide a maximum amount of information on biochemistry and morphology of a biological sample, a TPEF imaging platform should offer excitation and detection of multiple fluorophores.

SHG has lifetimes of the virtual state in the order of few femtoseconds. Hence, it prevents saturation that might pose a problem in TPEF microscopy where the excited electrons remain in the excited state for a few nanoseconds before returning to the ground state to be available for another excitation. In this non-resonant process two pump photons are annihilated and a single photon of twice the frequency is created. No molecules are excited to electronic of vibrational states and by that phototoxicity and photo-bleaching are prevented. Since SHG is energy conserving no non-radiative energy is lost during the relaxation of the excited state. Due to its sensitivity to molecular symmetry breaking SHG can be used to image collagen type I fibers, microtubules, and the highly polarizable myosin found in muscles, as these biological structures are assembled from fairly ordered, large non-centrosymmetric assemblies. Changes in the collagen arrangement can be a biomarker for pathological tissues [16]. The combination of TPEF and SHG provides information content comparable to standard hematoxylin -eosin (HE) stained slices in diseased or cancerous tissue.

CARS microscopy is a powerful method in biomedical imaging with molecular vibrational contrast for the wide range of biological materials that do not exhibit strong optical transitions to electronic states in the visible and NIR wavelength regime. CARS as third-order nonlinear process drives a vibrational transition in a molecule with two photons. A third photon probes the induced vibrational coherence of the molecule. The three two-color synchronized pulse trains are a pump beam of frequency ω_p, a Stokes beam of frequency ω_S and a probe beam at frequency $\omega_p r$. An energy difference between pump and Stokes beams that matches the energy gap of a particular vibrational transition drives the vibrational oscillators within the focus coherently in phase. The subsequent vibrational coherence is read out by additional scattering of the pump beam that generates a coherent radiation at the anti-Stokes frequency without any energy deposition in the molecule during the CARS process. Image contrast arises from a particular vibrational frequency. Spectral focusing CARS uses chirped laser trains for fast and easy switching of the vibrational excitation frequency. Image sequences containing spectroscopic information add an additional dimension compared to single color CARS. The frequency difference can be tuned by changing the optical delay. Spectral analysis based on multiple molecular vibrations allows for spatial discrimination of the molecular components in the sample [17], [18]. The applications of CARS range from label-free imaging of cells and cell activity [19] to imaging of tissues with the potential to replace current standard histological methods [20], [21].

Optimizing lasers for MPM is a challenging mission. Several interdependent parameters that can impact both sample and image quality have to be considered. The key is to design a laser for optimized excitation by providing the best balance among peak power, average power, and repetition rate. A high photon concentration confined in space and time is guaranteed from ultra-fast lasers with short pulse trains and high peak powers. In that way sufficient excitation powers with moderate time-averaged illumination doses can be achieved. Titanium doped sapphire is the most favorable gain medium as ultra-broadband solid-state laser material for ultrashort pulse generation. Its unrivalled emission bandwidth ranging from 650 to 1100 nm together with its excellent mechanical and thermal properties as well as high laser damage threshold are the key parameters for its success story in multimodal MPM. Light scattering and photo-damage effects are low in the NIR regime and water absorption is still tolerable to ensure imaging depths of more than 0.5 mm in tissue. With transient intensities of GW cm^{-2} and femtosecond pulse durations at repetition rates in the 70–100 MHz regime nonlinear signals can be efficiently generated with only mWs average laser power on the tissue. However, wide-spread applications in the life sciences with femtosecond Ti:sapphire lasers are hampered by the highly complex and expensive pump source with large footprint. Typically diode-pumped solid state lasers (DPSSL) or optically-pumped semiconductor lasers (OPSL) are used. Reduction in size, cost and complexity can be achieved by replacing such pump lasers with low-cost and compact laser diodes to increase the overall system efficiency. The first direct diode pumped continuous wave (cw) Ti:sapphire laser was introduced by Roth *et al.* in 2009 [22] and adapted for mode-locking with a SESAM device [22], [23] and Kerr-lens mode-locking [24].

Previously, we demonstrated a multimodal epi-detection nonlinear laser-scanning microscope (LSM) with a compact and cost-reduced femtosecond Ti:sapphire laser [25]. This system

featured simultaneous acquisition of signals arising from freshly excised mouse ear tissue with spectral focusing CARS, TPEF, and SHG, while the laser source still used a water-cooled frequency-doubled distributed Bragg reflector-tapered diode laser to pump the Ti:sapphire laser. A simpler and more cost-effective solution is required.

Recently, direct diode pumped femtosecond Ti:sapphire lasers with the potential for MPM were introduced [26], [27]. Despite the so far low output power and/or the limited SESAM lifetime, those direct diode pumped lasers have shown great potential in reducing the complexity and cost of the nonlinear bioimaging instruments. Therefore, further developments are expected to improve the oscillators and help widespreading the applications in multiphoton imaging as well as other directions.

In this paper, we introduce an in vivo multimodal multicolor non-linear optical imaging platform solely based on a new direct diode pumped femtosecond Kerr-Lens-mode-locked (KLM) Ti:sapphire oscillator and discuss the potential and technical details allowing for optimized excitation of multicolor TPEF, TPEF, SHG and CARS signals. The biomedical imaging performances are demonstrated in living organisms showing the potential for in vivo imaging.

II. Direct Diode Pumped Femtosecond Ti:Sapphire With Yb Fiber Amplifier Add-On

Briefly, the main light source is a direct diode-pumped ultrafast Ti:sapphire laser (VIULASE GmbH) with a nominal pulse repetition rate of 80 MHz and 440 mW mode-locked output power. The center wavelength is set at 805 nm with a spectral bandwidth of 15 nm (FWHM) for optimal combined spectral focusing CARS, multicolor TPEF and SHG microscopy. The dispersive mirror controlled ultrafast laser delivers a pulse energy of 5.5 nJ with a measured pulse duration of about 70 fs which corresponds to a peak power of 81 kW. We combined two commercially available individual emitters from Nichia operating at 462 nm with up to 2.9 W cw average power. In contrast to a recent paper from Jamal *et al.* [28], these diodes provide higher output powers allowing for stronger pumping. The detected RF pulse train is stable with no signs of mode-locking instabilities. In the same way, the RF spectrum exhibits a clean repetition rate tone, which is an indication for clean mode-locking operation. The beam quality, given by the parameter M^2, was measured for the x and y axis of the laser beam. For the calculation of M^2 we used the following procedure: first we identified the position of the Rayleigh range Z_R by using a CCD camera and a 200 mm lens. Then we calculated the imbedded Gaussian beam diameter d_0 using the relationship $d_0 = 2sqrt((Z_R\lambda)/\pi)$ and finally we obtained M^2 by using the relationship $M^2 = (D_m/d_0)^2$ with D_m as measured beam waist diameter. We repeated this procedure according to ISO standard 11 146. We finally calculated an M^2 factor of 1.07 and 1.14 for the horizontal and vertical axis, respectively. Beam divergence has been calculated to be <1 mrad by using a CCD camera and by measuring the beam waist at three different locations.

The noise performance of laser systems used for biomedical applications is one of the key points for imaging formation.

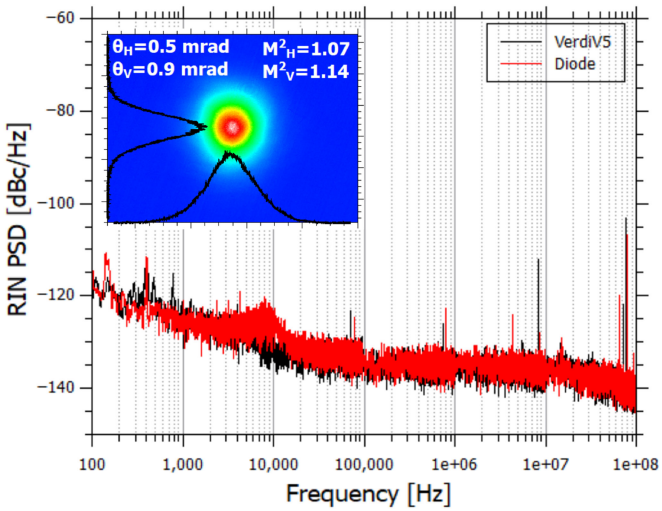

Fig. 1. Noise measurement results. Inset beam shape 11 cm away from the laser, divergence and M^2 measurement results.

Understanding of the noise components of a specific laser is not only helping to improve the image quality but also enables the realization of a better performing device. Hence, the identification of the origin of noise and the mechanisms of noise transfer in an optical system for bioimaging is of great importance. Here, we measured the amplitude noise of our direct diode pumped Ti:sapphire laser and compared it with a Ti:sapphire laser pumped by diode pumped solid-state laser (Verdi V, Coherent). It has been shown that the amplitude and envelope phase noise of a mode-locked laser depend directly on the pump laser amplitude stability [29]. The measurements are performed as follow: first the optical power of the laser under analysis is adjusted using a neutral density filter. The attenuated beam is detected using a fast photodetector having 1 ns rise time (Thorlabs DET10 A). The output current signal of the photodectector is directed to a transimpedence amplifier with 50 MHz bandwidth and a current to voltage gain factor of 0.5 mV/μA (Hamamatsu C6438-01). The obtained voltage signal is investigated using the FFT spectrum analyzer function of a 600 MHz lock-in amplifier (Zürich Instrument UHFLI 600 MHz) which is able to measure the amplitude modulation spectrum of the photoreceiver system (photodetector and transimpedence amplifier) giving a measure of the relative intensity noise (RIN) of the laser. Noise measurements showing the power spectral density (PSD) were performed in the range 100 Hz to 100 MHz by stitching 6 frequency scans together at 1 kHz, 10 kHz, 100 kHz, 1 MHz, and 10 MHz. The individual scans were performed with different resolution (measurement bandwidth) and keeping the number of FFT points fixed. The PSD is normalized using the procedure in Scott *et al.* [30] and Tawfieq *et al.* [31] in unit of dBc/Hz. The results are shown in Fig. 1. The rms value of the RIN is obtained by integrating the normalized PSD over a frequency interval [1MHz-100Hz]. The shotnoise limit is at -143 dB and the RIN rms is 0.0215% for the KLM Ti:sapphire pumped by a VerdiV5 and 0.0294% for our new direct diode-pumped Ti:sapphire. The peaks at 76 MHz and

80 MHz reveal the repetition rates of the lasers and harmonics are also visible. As shown in Fig. 1 the noise performance of both KLM Ti:sapphire lasers are comparable indicating that no additional noise is introduced by the direct diode-pumping scheme. Hence, the new laser shows great potential for in vivo biomedical imaging.

The high output average power allowed the splitting of the pulse train for generating synchronized two color pulses trains required for multicolor TPEF and spectral focusing CARS microscopy. Briefly, a 60:40 beam splitter divided the beam into two pulse trains. 176 mW are focused into a polarization-maintaining photonic crystal fiber (PCF) and a supercontinuum (SC) ranging from the visible to the NIR spectral region is generated as previously reported [25]. Excellent stability and spatial mode quality of the output mode-locked beam guaranteed sufficient SC generation and amplification. Single mode operation in time and spatial mode is assured by the imaging modalities and efficient PCF pumping.

To prevent disturbance of the mode-locking process due to backreflection from the PCF surface a Faraday isolator was inserted. 18 nm at full width at half maximum (FWHM) with 3 mW output are filtered at 1050 nm and subsequently amplified in an ytterbium-doped (Yb) fiber amplifier up to 100 mW. The 805 nm 264 mW output and the 1050 nm 100 mW output are compressed with two negative chirping units and subsequently stretched to 1 and 0.7 ps, respectively at the sample position in our LSM platform. The use of sub 100 fs pulse trains for MPM has shown a significant advantage compared to longer pulses (>100 fs) with a 1.5 to 2 fold increase of the TPEF signal. The Figure of Merit of TPEF imaging is degraded with longer pulses [32].

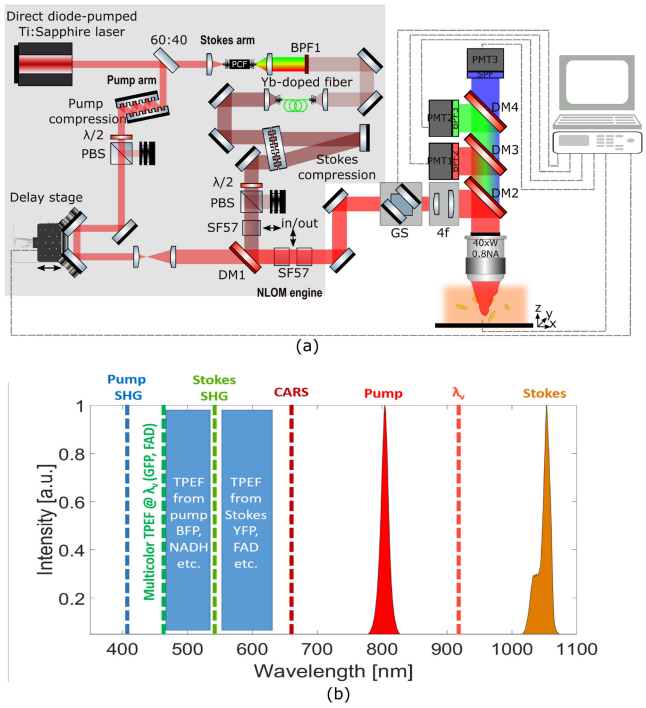

Fig. 2. (a) Multimodal nonlinear optical microscopy setup based on direct diode pumped Ti:Sapphire laser. BPF, band-pass filter; PMT, photomultiplier tube; DM, dichroic mirror; GM, galvanometric scanning mirrors. (b) Spectra of pump and Stokes beam and the relative excitation bandwidth of multiphoton absorption: SHG, two-photon absorption (TPEF) and CARS. By synchronizing pump and Stokes beams we create a virtual wavelength for two-photon multicolor excitation $\lambda_\nu = 2/(1/\lambda_{pump} + 1/\lambda_{Stokes})$ that corresponds to 911 nm.

III. Principle of Multimodal Multicolor Nonlinear Optical Microscopy

The basic configuration of the proposed multicolor two-photon excited fluorescence microscopy scheme is discussed here.Briefly, our multimodal multicolor non-linear optical imaging shown in Fig. 2(a) uses the direct diode pumped femtosecond Ti:sapphire laser in combination with the inherently synchronized high power Yb fiber amplifier for excitation as described in detail elsewhere [25]. In our previous work we used a distributed Bragg reflector (DBR)-tapered diode laser to pump a 125 MHz Ti:sapphire laser in a customized upright microscope and demonstrated the potential for TPEF, SHG and CARS. In this work, the 440 mW output of our direct diode pumped femtosecond Ti:sapphire laser was used to generate 264 mW output at 805 nm and 100 mW at 1050 nm. By using two synchronized pulse trains, an additional virtual two-photon excitation wavelength at 911 nm was generated. The two generated pulse trains were combined with a dichroic beam-splitter before entering the LSM. A computer controlled delay stage guaranteed the time overlap of the two beams at the focal plane on the sample and allowed for changing of the temporal overlap for fast tuning of the Raman frequency covering the CH stretching vibrations. Two negative chirping units composed of a set of dispersive mirrors and a grating pair were used to pre-compensate the group delay dispersion (GDD) caused by the microscope optics. Equal chirping of the pump and Stokes pulses was achieved by introducing a 5 cm long SF57 glass bock in the Stokes arm and a 10 cm long SF57 glass block in the combined beam path before entering the microscope enabling a spectral resolution for CARS spectroscopy of roughly ∼35 cm^{-1}. The scanning optics comprised a scan lens, a tube lens, and a set of galvanometric mirrors (6220H 8 mm, Cambridge Technology) that could scan two-dimensional field of view with a frame rate of about 1 frame per second (fps). The scanning light was directed into our customized inverted microscope (Zeiss Axio Observer) and focused on the specimen through a high numerical aperture (NA) objective lens (NIR Apo 40x, Nikon). A motorized three-axis scanning stage (PILine xy M687, PInano z P736, Physik Instrumente GmbH & Co. KG) was used to navigate the specimen to the targeted region of interest (ROI) and to acquire three-dimensional z-stacks via axial scanning.

The backscattered light signals were separated from the excitation beams with a dichroic beam-splitter and directed to a series of photomultiplier tubes. TPEF, SHG and CARS could be detected on a single PMT by using a combination dichroic mirrors and bandpass filters. Due to its nature, SHG was generated during multicolor two-photon excitation if a non-centrosymmetric structure was illuminated within the specimen. The red, green and blue detection channels were separated with two additional

TABLE I
MULTIMODAL MULTICOLOR EXCITED FLUOROPHORES

Localization	Fluorophore	Max multiphoton Ex/Em [nm]	Imaging modality
Mitochondrial matrix	NAD(P)H	730-820/ 460-480	TPEF (pump)
	FAD	750-1000/ 510-650	TPEF (multicolor)
ECM	Elastin	730-810/ 460-480	TPEF (pump)
	Collagen	800/400	SHG(pump)
Cell	Lipid droplets	805+1050/652 ($2850cm^{-1}$)	CARS
	Protein	805+1050/652 ($2850cm^{-1}$)	CARS
	DNA	805+1050/652 ($2850cm^{-1}$)	CARS
Protein conjugates	Rhodamine	780-860/ 520-590	TPEF (pump)
Gene expression	BFP	780-820/488	TPEF (pump)
	eGFP	900-920/516	TPEF (multicolor)
	YFP	860-1100/532	TPEF(Stokes+ multicolor)

dichroic mirrors and bandpass filters. SHG signal could be detected by using an emission filter (BrightLine FF01-400/50-25, Semrock) in front of the PMT in the blue channel. The spectral focusing CARS signal appears in the red channel and could be detected using an emission filter ((HQ640/50 m, Chroma) in front of the PMT. ScanImage 3.8 software [33] controls the galvanometer scanners and data acquisition in combination with a customized Matlab program. All imaging data were analyzed with the open source software ImageJ [34].

The multimodal multicolor platform shown in Fig. 2(a) allows for simultaneous and intrinsically co-registered detection of well-known biomarkers and optimal contrast for biomedical applications by using a single laser source. The frequency emission locations of the exogenous and endogenous fluorophores simultaneously addressable with our proposed platform are shown in Fig. 2(b) showing no spectral overlap. Table I provides an overview of interesting biomarker contrast addressable with the two synchronized pulse trains at 805 nm and 1050 nm and additionally a virtual two-photon excitation wavelength at 911 nm.

The pump beam could be used for SHG and TPEF imaging of blue/cyan fluorescence proteins (BFP/CFP) or intrinsic chromophores such as lipofuscin, melanin, phorphyrins, keratin and collagen in the blue channel. At the same way, the Stokes beam could be used for SHG and TPEF imaging of yellow fluorescent proteins (YFP) in the green channel. The green fluorescent protein (GFP) is one of the most commonly applied fluorophores in fluorescence microscopy because of the fact that the GFP gene can be introduced and expressed in a wide range of biological species as intrinsic label of specific cells. We optimized our two excitation beams to target in vivo and live cell GFP imaging by negating the need for extrinsic fluorophores that can be phototoxic. Pump and Stokes beams were coherently and simultaneously used for CARS imaging of lipid and protein molecules and for multicolor TPEF excitation of GFP. Indeed, the wavelength mixing of pump and Stokes beams and by that additionally generated virtual two-photon excitation wavelength at 911 nm allowed for TPEF excitation of GFP.

Endogenous fluorophores such as NADH and FAD play an important role in physiological processes and can be used as intrinsic biomarkers in living tissue. As primary intracellular source they are the two major components of redox reactions in the cell and central regulators of energy production and metabolism [35]. Since their fluorescence is linked to the metabolic activity of cells, it assesses physiological processes such as stem cell differentiation, early cancer progression and neurodegenerative diseases. In our approach NADH and FAD signals could be obtained simultaneously and with intrinsic co-registration free of motion artifacts in living tissue circumventing problems associated with differences in absorption spectra and disparity in concentration. NADH was excited at 805 nm and detected in the blue channel. The FAD signal was provided via the additional equivalent two-photon excitation wavelength at 911 nm. Switching between the different modalities was performed by a flip mount.

IV. APPLICATION OF MULTIMODAL MULTICOLOR NONLINEAR OPTICAL MICROSCOPY

A. Multicolor TPEF Microscopy

We verified the multicolor TPEF imaging capabilities of our platform on green fluorescent dragon beads (FSDG009, Bangs Laboratories, Inc.). Multicolor TPEF excitation was achieved by synchronizing pump and Stokes beams to obtain the virtual two-photon excitation wavelength λ_ν at 911 nm. One photon from the pump and one photon from the Stokes beams were simultaneously absorbed thus producing fluorescence at a wavelength just longer than half of λ_ν. Experimental checks on the collected fluorescence signal to understand its origin were performed and shown in Fig. 3. The power dependency and the excitation beams time overlap dependence of the signal of a single bead (white arrows in Fig. 4) were evaluated. Indeed, linear dependencies of the fluorescent signal have been found for pump and Stokes intensities (see Fig. 3(b), respectively. R-squared of the linear fit for the pump were 0.9983 and for the Stokes 0.9965, respectively. Moreover, the detected signal disappears when pump and/or Stokes beams were unsynchronized or blocked. TPEF contribution from the pump beam only was still visible and was represented by the DC component of the plot in Fig. 3(a). Hence, the collected signal was assigned as fluorescent contribution of green dragon beads by means of multicolor TPEF. Multicolor TPEF images from green dragon beads were acquired with 6.4 μs pixel dwell time, 256×256 pixels. The pump and Stokes powers at the imaging plane were 40 mW and 24 mW, respectively Unsynchronized pulses did not significantly contribute to the two-photon fluorescence signal as shown in Fig. 4(b), while synchronized pulses exhibit a strong two-photon fluorescence signal.

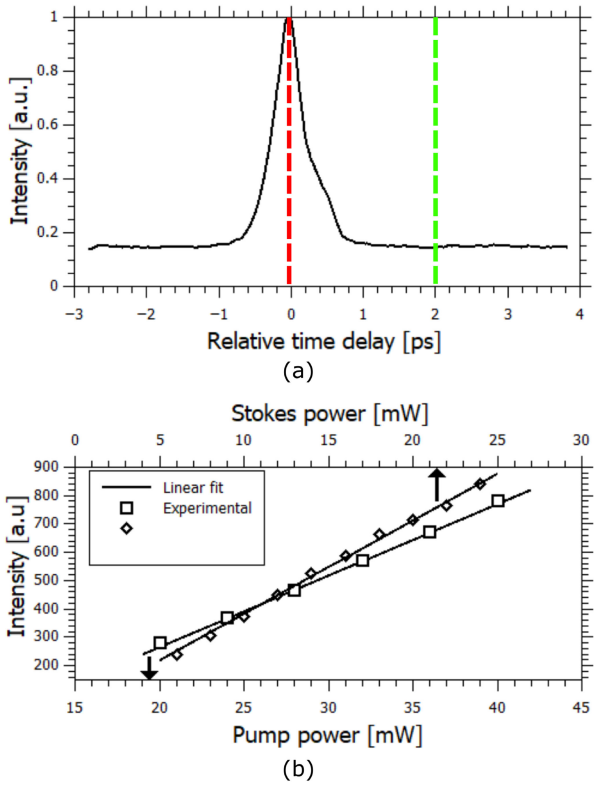

Fig. 3. Green dragon beads measurements results. (a) Measured spectral intensity signal of the beads indicated with white arrows in Fig. 4. For synchronized pulses (red dashed line) and unsynchronized pulses (green dashed line). (b) Power dependency measurements with fixed pump power at 40 mW and varying Stokes power and vice versa with fixed Stokes power at 24 mW and varying pump power.

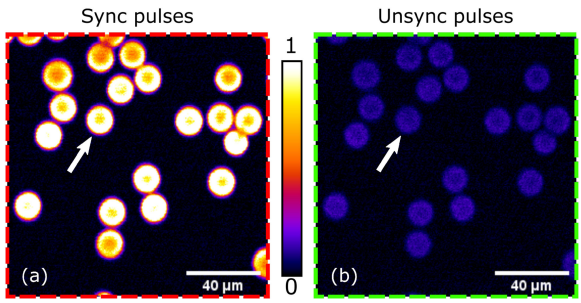

Fig. 4. Green dragon beads imaging results when pump and Stokes pulses are synchronized (a) and unsynchronized (b). White arrows indicates the beads used to produce the spectral intensity signal in Fig. 3(a) and the power study in Fig. 3(b).

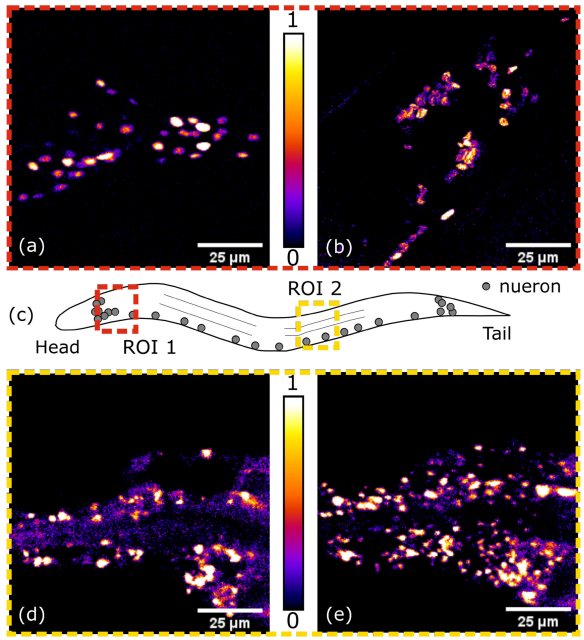

Fig. 5. Results of in vivo multicolor TPEF imaging of *C. elegans*. The *C. elegans* strains used for imaging were ZIM1229; mzmEx749; (mzmEx749 = [unc-31::2xSV40NLS::YFP::egl-13NLS]). (a) *C. elegans* with with nuclear localized YFP expressing neurons imaged at the position of the head with 1050 nm beam. (b) *C. elegans* with with nuclear localized BFP expressing neurons imaged at 800 nm. (c) *C. elegans* sketch. (d) wild type *C. elegans* revealing NADH at the position of the gut imaged at 800 nm. (e) wild type *C. elegans* revealing FAD at the position of the gut imaged with multicolor TPEF.

B. Caenorhabditis Elegans

Caenorhabditis elegans as small free-living hermaphroditic, nematode worm completes a life cycle in 2.5 days at 25 °C. Its transparent nature makes it extremely interesting for MPM investigation. Together with the broad range of genetic and molecular tools available *C. elegans* allows to gain unique insight into fundamental problems in biology.

Fig. 5 shows results of in vivo multicolor TPEF imaging combining contrast from endogenous as well as exogenous fluorophores. MPM images were acquired with 6.4 μs pixel dwell time, 256 $\times$ 256 pixels. The pump and Stokes powers at the imaging plane were 25 mW and 15 mW, respectively. Before imaging, *C. elegans* transgenically expressing nuclear localized BFP or YFP in all neurons were immobilized in s-basal with 1 μM tetramizol mounted in a PDMS chip [36] and positioned on the sample plane of the LSM.

Fig. 5(a) reveals YFP and Fig. 5(b) BFP expressing neurons on the head region of a living *C. elegans* by using the 1050 nm Stokes and 805 nm pump beam only for excitation, respectively. Fig. 5(c) and (d) reveal metabolic information. NADH image is created at the gut position of a living *C. elegans* excited at 800 nm and the corresponding FAD image was created with multicolor excitation by using the virtual wavelength λ_ν significantly contribute to the two-photon fluorescence signal as shown in Fig. 4(b), while synchronized pulses exhibit a strong two-photon fluorescence signal.

C. Zebrafish Larvae

Zebrafish (*Danio Rerio*) as research model has gained significant popularity in the last few decades [37], [38]. Its transparency at embryonic and larval stages, amenability for genetic manipulation and its rapid developmen tmake it unmatched to other research models and accessible for MPM. Moreover, the zebrafish genome has been sequenced [37], showing that 70% of human genes can be found in the zebrafish and 84% of the human disease related genes have a zebrafish counterpart, making it a

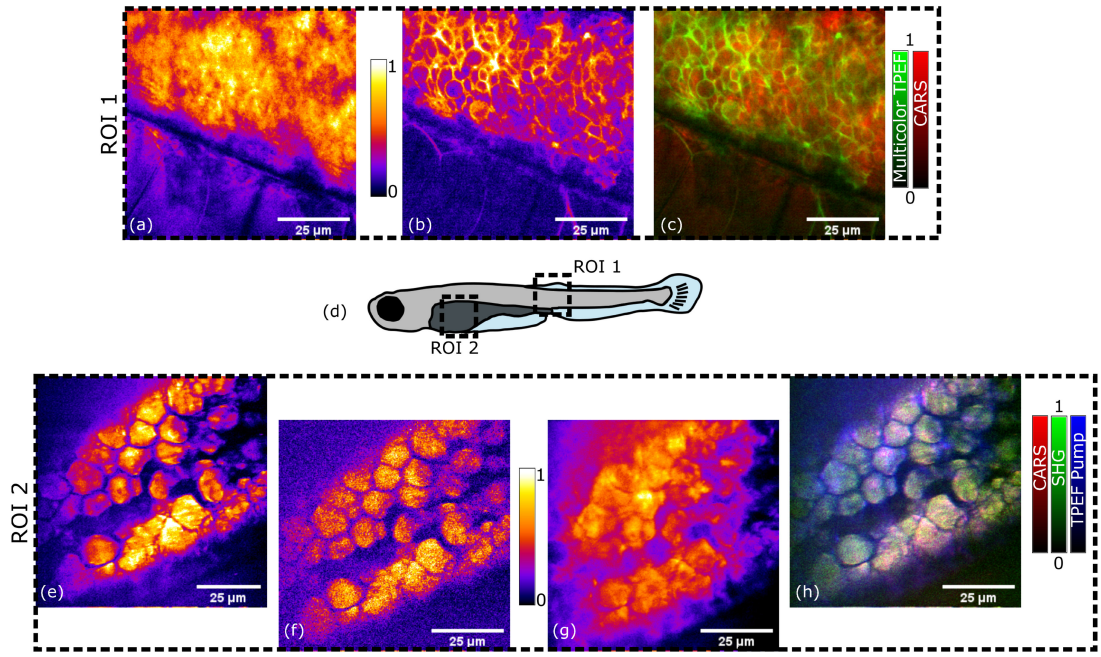

Fig. 6. In vivo multimodal multicolor imaging results of 5dpf zebrafish transformed larvae. (a) CARS image at ROI 1 reveals lipid distribution within the tumor area. (b) GFP fluorescent signal from transformed cell membrane obtained through multicolor TPEF of ROI 1. (c) pseudocolor merged image. (d) zebrafish larvae. (e) CARS image of yolk sac revealing lipid content (f) SHG image of yolk sac revealing collagen composition and (g) TPEF image of yolk sac revealing elastin composition. (h) A pseudocolor merged image is presented to show the complementarity of the CARS, TPEF and SHG signals.

promising model to study human diseases including cancer [39] and offering a cost-effective and high throughput model for in vivo large-scale drug screening [40].

By using transgenic fluorescence lines or by looking at endogenous markers, optical microscopy can objectively and non-invasively identify, evaluate and assess changes between healthy and pathological state. We use a zebrafish cancer model to investigate the tumor microenvironment in zebrafish larvae in vivo. In our transgenic model tumorigenesis is induced by expression of an oncogene fused to GFP and targeted to the cell membrane of cells in the spinal cord. Fig. 6 shows the conducted in vivo zebrafish measurements. Eggs from oncogene-expressing zebrafish were maintained in E3 medium at 28 °C under standard conditions. 1-phenyl 2-thiourea (PTU) was added to the medium between 22 and 24 hours-post-fertilization (hpf) to suppress pigmentation. 5 d-post-fertilization (dpf) old zebrafish larvae were anesthetized in 100 mg/L tricaine methanesulfonate and immobilized in 1% ultra-low gelling temperature agarose at 32 °C. We imaged the zebrafish tumor microenvironment in vivo by combining spectral focusing CARS, SHG, multicolor TPEF and TPEF imaging. Images were acquired with 6.4 μs pixel dwell time, 256 × 256 pixels. The pump and Stokes powers at the imaging plane were 25 mW and 15 mW, respectively. Increased lipid concentrations within regions harboring transformed cells is shown in the CARS image due to higher cell density caused by hyperproliferation (Fig. 6(a)). The lipid content is heavily augmented in the neural tissue invading the muscle region and the expected well-organized myotomes structure is not visible anymore. GFP fluorescent signals from hyperproliferative cell membranes obtained through multicolor TPEF shown in Fig. 6(b) verify the origin of the corrupted signal. In the merged intrinsic co-registered representation (Fig. 6(c)) the cell membrane of the hyperproliferative cells and the increased lipid content investigated at 2860 cm^{-1} perfectly match. In addition, CARS (Fig. 6(e)), SHG (Fig. 6(f)) and TPEF (Fig. 6(g)) images excited at 805 nm reveal the content of nutrients within the yolk sac. Lipids, collagen and elastin are the major sources of contrast. The images show a strong compositional heterogeneity. CARS could be potentially used to study the vertebrate lipid transport and metabolism by injection of fatty acids into the zebrafish yolk to study risk factors for coronary artery disease.

V. Conclusion

In conclusion, it has been demonstrated that a direct diode pumped femtosecond KLM Ti:sapphire laser can be used in combination with a PCF and fiber amplifier to perform in vivo bioimaging. The combination of high peak power, GVD precompensation and possible fiber delivery of the laser [41] outperforms conventional Ti:sapphire and fiber lasers in multimodal multicolor MPM applications while simultaneously offering a smaller form factor with reduced maintenance and overall up to 10 times lower cost of ownership. The key requirements for live tissue imaging can be met with our multimodal multicolor platform where all signals are acquired in the backward direction. The laser was optimized in terms central wavelength and bandwidth as well as pulse duration and repetition rate. Long penetration depths can be obtained with low photo-damage. Reasonable imaging speeds allow for real-time visualization. The ability to multiplex signals from different emission spectra, and potential for high spatial resolution and real-time display

provide substantial advantages over conventional imaging techniques. The present work implemented and demonstrated an efficient and affordable method for simultaneous and intrinsic co-registered investigation of several exogenous and endogenous fluorophores with different absorption spectra within a single measurement along with SHG and spectral focusing CARS. Multiple contrast including structural, molecular and biochemical information with high sensitivity and specificity is provided and can potentially address a wide variety of unmet clinical needs for disease detection, localization and better understanding. One significant difference compared with previous reported multicolor approaches is the combination with spectral focusing CARS adding highly specific molecular and spectroscopic information on a cellular level. Indeed, a stable SC could be obtained to create the inherently synchronized Stokes beam centered at 1050 nm featuring TPEF imaging. Multicolor TPEF imaging with an additional virtual two-photon excitation wavelength at 911 nm and spectral focusing CARS spectroscopy and imaging make our approach extremely interesting for depth enhanced multimodal GFP imaging. It can be performed by the combination of these synchronized pulse trains. In vivo *C. elegans* and zebrafish metabolic imaging demonstrate the potential of the platform towards automated image screening with possible automated feature detection as high-throughput imaging assay.

References

[1] L. Shi *et al.*, "Optical imaging of metabolic dynamics in animals," *Nat. Commun.*, vol. 9, no. 1, Dec. 2018.

[2] M. M. Kim, A. Parolia, M. P. Dunphy, and S. Venneti, "Non-invasive metabolic imaging of brain tumours in the era of precision medicine," *Nat. Rev. Clin. Oncol.*, vol. 13, no. 12, pp. 725–739, Dec. 2016.

[3] W. Denk, J. Strickler, and W. Webb, "Two-photon laser scanning fluorescence microscopy," *Science*, vol. 248, no. 4951, pp. 73–76, Apr. 1990.

[4] C. Xu, W. Zipfel, J. B. Shear, R. M. Williams, and W. W. Webb, "Multiphoton fluorescence excitation: New spectral windows for biological nonlinear microscopy," in *Proc. Nat. Acad. Sci.*, vol. 93, no. 20, pp. 10 763–10 768, Oct. 1996.

[5] W. R. Zipfel, R. M. Williams, R. Christie, A. Y. Nikitin, B. T. Hyman, and W. W. Webb, "Live tissue intrinsic emission microscopy using multiphoton-excited native fluorescence and second harmonic generation," in *Proc. Nat. Acad. Sci.*, vol. 100, no. 12, pp. 7075–7080, Jun. 2003.

[6] A. Zumbusch, G. R. Holtom, and X. S. Xie, "Three-dimensional vibrational imaging by coherent anti-stokes raman scattering," *Phys. Rev. Lett.*, vol. 82, no. 20, pp. 4142–4145, May 1999.

[7] W. R. Zipfel, R. M. Williams, and W. W. Webb, "Nonlinear magic: Multiphoton microscopy in the biosciences," *Nat. Biotechnol.*, vol. 21, no. 11, pp. 1369–1377, Nov. 2003.

[8] C. L. Evans, E. O. Potma, M. Puoris'haag, D. Cote, C. P. Lin, and X. S. Xie, "Chemical imaging of tissue in vivo with video-rate coherent anti-stokes raman scattering microscopy," in *Proc. Nat. Acad. Sci.*, vol. 102, no. 46, pp. 16 807–16 812, Nov. 2005.

[9] M. Ji *et al.*, "Detection of human brain tumor infiltration with quantitative stimulated raman scattering microscopy," *Sci. Transl. Med.*, vol. 7, no. 309, pp. 309ra 163–309ra163, Oct. 2015.

[10] D. R. Rivera *et al.*, "Compact and flexible raster scanning multiphoton endoscope capable of imaging unstained tissue," in *Proc. Nat. Acad. Sci.*, vol. 108, no. 43, pp. 17 598–17 603, Oct. 2011.

[11] J. Hou, J. Williams, E. L. Botvinick, E. O. Potma, and B. J. Tromberg, "Visualization of breast cancer metabolism using multimodal nonlinear optical microscopy of cellular lipids and redox state," *Cancer Res.*, vol. 78, no. 10, pp. 2503–2512, May 2018.

[12] P. Mahou *et al.*, "Multicolor two-photon tissue imaging by wavelength mixing," *Nat. Methods*, vol. 9, no. 8, pp. 815–818, Aug. 2012.

[13] C. Stringari *et al.*, "Multicolor two-photon imaging of endogenous fluorophores in living tissues by wavelength mixing," *Sci. Rep.*, vol. 7, no. 1, Dec. 2017.

[14] H. Segawa, M. Okuno, H. Kano, P. Leproux, V. Couderc, and H.-o. Hamaguchi, "Label-free tetra-modal molecular imaging of living cells with CARS, SHG, THG and TSFG (coherent anti-stokes raman scattering, second harmonic generation, third harmonic generation and third-order sum frequency generation)," *Opt. Exp.*, vol. 20, no. 9, Apr. 2012, Art. no. 9551.

[15] K. Guesmi *et al.*, "Dual-color deep-tissue three-photon microscopy with a multiband infrared laser," *Light: Sci. Appl.*, vol. 7, no. 1, Dec. 2018.

[16] E. Brown *et al.*, "Dynamic imaging of collagen and its modulation in tumors in vivo using second-harmonic generation," *Nat. Med.*, vol. 9, no. 6, pp. 796–800, Jun. 2003.

[17] A. F. Pegoraro, A. Ridsdale, D. J. Moffatt, Y. Jia, J. P. Pezacki, and A. Stolow, "Optimally chirped multimodal CARS microscopy based on a single ti:sapphire oscillator," *Opt. Exp.*, vol. 17, no. 4, p. 2984, Feb. 2009.

[18] T. Hellerer, A. M. Enejder, and A. Zumbusch, "Spectral focusing: High spectral resolution spectroscopy with broad-bandwidth laser pulses," *Appl. Phys. Lett.*, vol. 85, no. 1, pp. 25–27, Jul. 2004.

[19] Z. Zhang, "Label-free multiphoton microscopy promises real-time optical molecular imaging of live tissues,"*Scilight.*, vol. 2019, no. 40, p. 401103, Oct. 2019.

[20] C. W. Freudiger *et al.*, "Multicolored stain-free histopathology with coherent raman imaging," *Lab. Investigation*, vol. 92, no. 10, pp. 1492–1502, Oct. 2012.

[21] H. Tu *et al.*, "Stain-free histopathology by programmable supercontinuum pulses," *Nat. Photon.*, vol. 10, no. 8, pp. 534–540, Aug. 2016.

[22] P. W. Roth, A. J. Maclean, D. Burns, and A. J. Kemp, "Directly diode-laser-pumped ti:sapphire laser," *Opt. Lett.*, vol. 34, no. 21, Nov. 2009, Art. no. 3334.

[23] P. W. Roth, A. J. Maclean, D. Burns, and A. J. Kemp, "Direct diode-laser pumping of a mode-locked ti:sapphire laser," *Opt. Lett.*, vol. 36, no. 2, Jan. 2011, Art. no. 304.

[24] C. G. Durfee *et al.*, "Direct diode pumped kerr lens modelocked ti:sapphire laser oscillator," in *Proc. Conf. Lasers Electro-Opt.*, vol. 20, no. 13, 2012, p. 13677. [Online]. Available: https://www.osapublishing.org/oe/abstract.cfm?uri=oe-20-13-13677.

[25] M. Andreana *et al.*, "Epi-detecting label-free multimodal imaging platform using a compact diode-pumped femtosecond solid-state laser," *J. Biomed. Opt.*, vol. 22, no. 9, pp. 1–7, Aug. 2017.

[26] M. D. Young, S. Backus, C. Durfee, and J. Squier, "Multiphoton imaging with a direct-diode pumped femtosecond ti:sapphire laser," *J. Microsc.*, vol. 249, no. 2, pp. 83–86, Feb. 2013.

[27] A. Rohrbacher, O. E. Olarte, V. Villamaina, P. Loza-Alvarez, and B. Resan, "Multiphoton imaging with blue-diode-pumped SESAM-modelocked ti:sapphire oscillator generating 5 nJ 82 fs pulses," *Opt. Exp.*, vol. 25, no. 9, May 2017, Art. no. 10677.

[28] M. Tahir jamal, A. K. Hansen, M. Tawfieq, P. E. Andersen, and O. B. Jensen, "Influence of pump beam shaping and noise on performance of a direct diode-pumped ultrafast ti:sapphire laser," *Opt. Exp.*, vol. 28, no. 21, Oct. 2020, Art. no. 31754.

[29] R. P. Scott, T. D. Mulder, K. A. Baker, and B. H. Kolner, "Amplitude and phase noise sensitivity of modelocked ti:sapphire lasers in terms of a complex noise transfer function," *Opt. Exp.*, vol. 15, no. 14, 2007, Art. no. 9090.

[30] R. Scott, C. Langrock, and B. Kolner, "High-dynamic-range laser amplitude and phase noise measurement techniques," *IEEE J. Sel. Topics Quantum Electron.*, vol. 7, no. 4, pp. 641–655, Sep. 2001.

[31] M. Tawfieq, A. K. Hansen, O. B. Jensen, D. Marti, B. Sumpf, and P. E. Andersen, "Intensity noise transfer through a diode-pumped titanium sapphire laser system," *IEEE J. Quantum Electron.*, vol. 54, no. 1, pp. 1–9, Feb. 2018.

[32] B. Resan *et al.*, "Two-photon fluorescence imaging with 30 fs laser system tunable around 1 micron," *Opt. Exp.*, vol. 22, no. 13, pp. 16456–16461, Jun. 2014.

[33] T. A. Pologruto, B. L. Sabatini, and K. Svoboda, "ScanImage: Flexible software for operating laser scanning microscopes," *BioMed. Eng. OnLine*, vol. 2, no. 1, Dec. 2003.

[34] J. Schindelin *et al.*, "Fiji: An open-source platform for biological-image analysis," *Nat. Methods*, vol. 9, no. 7, pp. 676–682, Jul. 2012.

[35] B. Chance, P. Cohen, F. Jobsis, and B. Schoener, "Intracellular oxidation-reduction states in vivo," *Sci.*, vol. 137, no. 3531, pp. 660–660, Aug. 1962, publisher: American Association for the Advancement of Science Section: Corrections and Clarifications.

[36] N. Chronis, M. Zimmer, and C. I. Bargmann, "Microfluidics for in vivo imaging of neuronal and behavioral activity in caenorhabditis elegans," *Nat. Methods*, vol. 4, no. 9, pp. 727–731, Sep. 2007.

[37] K. Howe *et al.*, "The zebrafish reference genome sequence and its relationship to the human genome," *Nature*, vol. 496, no. 7446, pp. 498–503, Apr. 2013.

[38] "Zfin the Zebrafish Information Network," Accessed Mar. 01, 2020. [Online]. Available: http://zfin.org/, .
[39] M. C. Mione and N. S. Trede, "The zebrafish as a model for cancer," *Dis. Models Mechanisms*, vol. 3, no. 9–10, pp. 517–523, Sep. 2010.
[40] S. Ridges *et al.*, "Zebrafish screen identifies novel compound with selective toxicity against leukemia," *Blood*, vol. 119, no. 24, pp. 5621–5631, Jun. 2012.
[41] M. Andreana, T. Le, W. Drexler, and A. Unterhuber, "Ultrashort pulse kagome hollow-core photonic crystal fiber delivery for nonlinear optical imaging," *Opt. Lett.*, vol. 44, no. 7, Apr. 2019, Art. no. 1588.

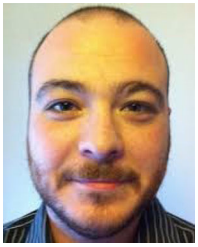

Marco Andreana was born in Brescia, Italy, in 1981. He received the M.Sc. dgeree in telecommunication engineering from the University of Brescia, Brescia, Italy, in 2008, and the dual Ph.D. degrees in electronic instrumentation and optoelectronics from the University of Brescia, Brescia, Italy, and the University of Limoges, Limoges, France, in 2011. He was with Xlim Research Institute, University of Limoges, where he worked on fiber and solid-state nonlinear optics, and in March 2012, he joined Molecular Photonics Group, Ottawa, ON, Canada, where he worked on stabilizing laser systems and CARS. He is currently working with the Medical University of Vienna, Vienna, Austria, where his currents research focuses on biomedical applications, especially in the field of nonlinear microscopy and OCT. His research interests include nonlinear optics and biophotonics.

Caterina Sturtzel received the Diploma degree in molecular biology from the University of Vienna, Vienna, Austria, and the Ph.D. degree as a shared project between the University of Vienna and the Medical University of Vienna. In 2014, she was a Postdoc and helped to establish the ZANDR platform with CCRI, where she is currently working as an Operator.

Ming Yang was born in Nanjing, China, in 1979. He received the master's degree from the Shanghai Institute of Optics and Fine Mechanics, Shanghai, China, in 2007 and the Ph.D. degree from the Max Born Institute for Nonlinear Optics and Short Pulse Spectroscopy, Berlin, Germany, in 2012. He joined the team of Femtolasers Produktion GmbH. He is currently one of the Co-founders of the VIULASE GmbH.

Richard Latham is currently a Research Technician with Zimmer lab.

Rainer A. Leitgeb (Member, IEEE) received the Ph.D. degree in theoretical physics from TU Wien, Vienna, Austria, in 1998. Since 2003, he has been a Professor of medical physics, and since 2014, he has beeen the Head of the Christian Doppler Laboratory of Innovative Optical Imaging and its Translation to Medicine, Medical University of Vienna. He spent three years as a Visiting Professor with EPFL Lausanne, Lausanne, Switzerland, and was a Visiting Professor with CNRS FEMTO-ST, Besancon, France. He has authored more than 200 publications including book chapters and patents. His research interests include functional, multimodal biomedical optical imaging, and advanced image processing aiming at their translation to medicine. He is a Fellow of SPIE and OSA.

Wolfgang Drexler was born in Vienna, Austria, in 1966. He received the M.S. and Ph.D. degrees in electrical engineering from Technische Universität Wien, Vienna, in 1991. From 1991 to 1998, he was an Assistant Professor with the Institute of Medical Physics, University of Vienna, Vienna, and from 1998 to 1999, a Research Associate with MIT, Cambridge, MA, USA. Between 2000 and 2006, he was an Associate Professor with the Institute of Medical Physics, University of Vienna, and between 2006 and 2009, a Full Professor (Distinguished Research Professor) of biomedical imaging, the Head of the Biomedical Imaging Group, and the Director of Research with Cardiff University, Wales, U.K. Since 2009, he has been a Full Professor of medical physics and the Head of the Center for Medical Physics and Biomedical Engineering, Medical University of Vienna, Vienna and since 2010, he has been the Honorary Distinguished Professor with Cardiff University.

Manuel Zimmer received the Ph.D. degree from the Max Planck Institute of Neurobiology, Munich, Germany. He visited the University of California, San Francisco, San Francisco, CA, USA, and Rockefeller University, New York, NY, USA, for his Postdoctoral Research. He founded his own group in 2010 with the Research Institute of Molecular Pathology, Vienna, Austria, and since 2018, he has been a University Professor of Neurobiology with the University of Vienna, Vienna.

Tuan Le received the Physics Diploma and the Ph.D. degree from the Vienna University of Technology, Vienna, Austria. Since 1998, he has been working in the field of femtosecond lasers. His research interests include the development of ultrafast lasers, short pulse fiber delivery, ultrafast optics, and applications of femtosecond laser pulses. He is a Co-Founder of VIULASE GmbH.

Martin Distel received the Ph.D. degree in neurobiology from Helmholtz Center, Munich, Germany. He is currently a Molecular Biotechnologist with the Technical University of Munich, Munich, and Lund's University, Lund, Sweden. He received Postdoctoral training from the University of California San Diego, San Diego, CA, USA. During his Ph.D. and Postdoc, he was using zebrafish as a model organism. Since 2014, he has been the Group Leader with CCRI and the Head of the ZANDR. His main research interests include cancer modeling in zebrafish using innovative genetic and xenografting approaches, live microscopy, and small compound screening on zebrafish disease models.

Angelika Unterhuber was born in Vienna, Austria, in 1971. She received the M.Sc. degree in technical physics from the Technische Universität Wien, Vienna, Austria, in 1998 and the Ph.D. dgeree in electrical engineering in 2006. From 1998 to 2002, she was the Product Manager for oscillators with Femtolasers Produktions GmbH. In 2006, she joined the School of Optometry and Vision Sciences, Cardiff University, as a Research Assistant. She returned to Vienna with a Marie Curie Fellowship. She is currently an Associate Professor with the Medical University of Vienna, Vienna. Her current research interests include multimodal biomedical imaging, including optical coherence tomography, nonlinear optical microscopy, and Raman-based technologies with a special focus on lasers and their translation to biomedical applications.